Neuron, Vol. 33, 1085–1097, September 12, 2002, Copyright ©2002 by Cell Press

A Membrane Marker Leaves Synaptic Vesicles in Milliseconds after Exocytosis in Retinal Bipolar Cells

David Zenisek,[1,4] Jürgen A. Steyer,[2] Morris E. Feldman,[3] and Wolfhard Almers[1,5]
[1]Vollum Institute
Oregon Health and Science University
Portland, Oregon 97201
[2]Department of Biology
University of California
Berkeley, California 94720
[3]Department of Biomedical Sciences
Cornell University
Ithaca, New York 14853
[4]Department of Cellular and Molecular Physiology
Yale University School of Medicine
SHM-B103
New Haven, Connecticut 06520

Summary

Perhaps synaptic vesicles can recycle so rapidly because they avoid complete exocytosis, and release transmitter through a fusion pore that opens transiently. This view emerges from imaging whole terminals where the fluorescent lipid FM1-43 seems unable to leave vesicles during transmitter release. Here we imaged single, FM1-43-stained synaptic vesicles by evanescent field fluorescence microscopy, and tracked the escape of dye from single vesicles by watching the increase in fluorescence after exocytosis. Dye left rapidly and completely during most or all exocytic events. We conclude that vesicles at this terminal allow lipid exchange soon after exocytosis, and lose their dye even if they connected with the plasma membrane only briefly. At the level of single vesicles, therefore, observations with FM1-43 provide no evidence that exocytosis of synaptic vesicles is incomplete.

Introduction

Under maintained stimulation, small synaptic terminals would soon exhaust their store of vesicles if it were not refilled with new ones. Because new vesicles require membrane gained through endocytosis, they can be made no faster than the endocytic retrieval of the requisite plasma membrane. This problem is most acute in the small synaptic terminals found in the brain. Indeed, synaptic terminals of hippocampal neurons have a rapid mechanism that can retrieve the membrane of vesicles with an estimated time constant of 1 s in some experiments (Pyle et al., 2000; but see also Sankaranarayanan and Ryan, 2000). In endocrine cells, endocytosis can be similarly fast (reviewed in Henkel and Almers, 1996).

Classical work holds that synaptic vesicles complete their exocytosis by flattening into the cell surface, and that the membrane thus added is retrieved by clathrin-mediated endocytosis (Heuser and Reese, 1973). However, flattening vesicle profiles failed to accumulate during vigorous transmitter release in some studies (Torri-Tarelli et al., 1985), and the complete cycle of exocytosis and clathrin-mediated endocytosis seemed too slow to explain the rapid membrane retrieval often found in later experiments. Therefore several authors have proposed alternative mechanisms (Meldolesi and Ceccarelli, 1981; Thomas et al., 1994; Kavalali et al., 1999) sometimes called "kiss-and-run" exocytosis when applied to synaptic vesicles (Valtorta et al., 2001). The essence of these mechanisms is that exocytosis is incomplete in proceeding no further than the opening of a fusion pore connecting the vesicle to the outside world. After allowing the escape of transmitter or hormone, the fusion pore closes again, and the remaining intact vesicle cavity is ready for refilling and re-use as a synaptic vesicle, or for degradation and processing in the case of dense core granules. Indeed, capacitance recordings on endocrine cells show that the fusion of single granules is reversible, either in the minority (Fernandez et al., 1984; Spruce et al., 1990; Albillos et al., 1997) or the majority of fusions (Ales et al., 1999). A granule can discharge all of its catecholamine while it transiently opens its fusion pore (Albillos et al., 1997; Ales et al., 1999). These observations strongly support incomplete exocytosis in endocrine cells.

Similar measurements have been difficult in synaptic terminals with their much smaller vesicles. Instead, the strongest case for incomplete exocytosis (or kiss-and-run) rests on measurements with styryl dyes such as FM1-43 and FM2-10 that fluoresce when they reversibly partition into lipid bilayers and selectively stain synaptic vesicles in intact terminals (Betz and Bewick, 1992; Ryan et al., 1993). A key finding is taken as evidence for kiss-and-run. During stimulation, stained hippocampal terminals lose FM2-10 more readily than the more hydrophobic FM1-43 (Klingauf et al., 1998; Kavalali et al., 1999; Pyle et al., 2000, but see Ryan et al., 1996). Since FM2-10 desorbs from plasma membranes faster than FM1-43, it was concluded that styryl dyes must desorb before they can leave a vesicle, and that synaptic vesicles close their fusion pore in seconds before all their FM1-43 can escape. A further implication is that synaptic vesicles are unable to exchange lipid with the plasma membrane (Klingauf et al., 1998; Kavalali et al., 1999) because any such exchange would allow dye to leave vesicles before it can desorb. Kiss-and-run exocytosis was reported also in hippocampal neurons stimulated with hypertonic sucrose where most vesicles apparently released their transmitter without losing styryl dyes. Neurons so stimulated were not even capable of taking up styryl dyes while they released transmitter (Stevens and Williams, 2000).

Exocytosis without lipid exchange would have important implications also for the mechanism of membrane fusion, a fundamental process whose final steps remain unknown. SNARE proteins are thought to mediate fusion by forcing vesicle and plasma membrane so close together that their lipid bilayers fuse of their own accord. If the resulting fusion pore is purely lipidic, as is widely believed (Jahn and Südhof, 1999), then lipids including

[5]Correspondence: almersw@ohsu.edu

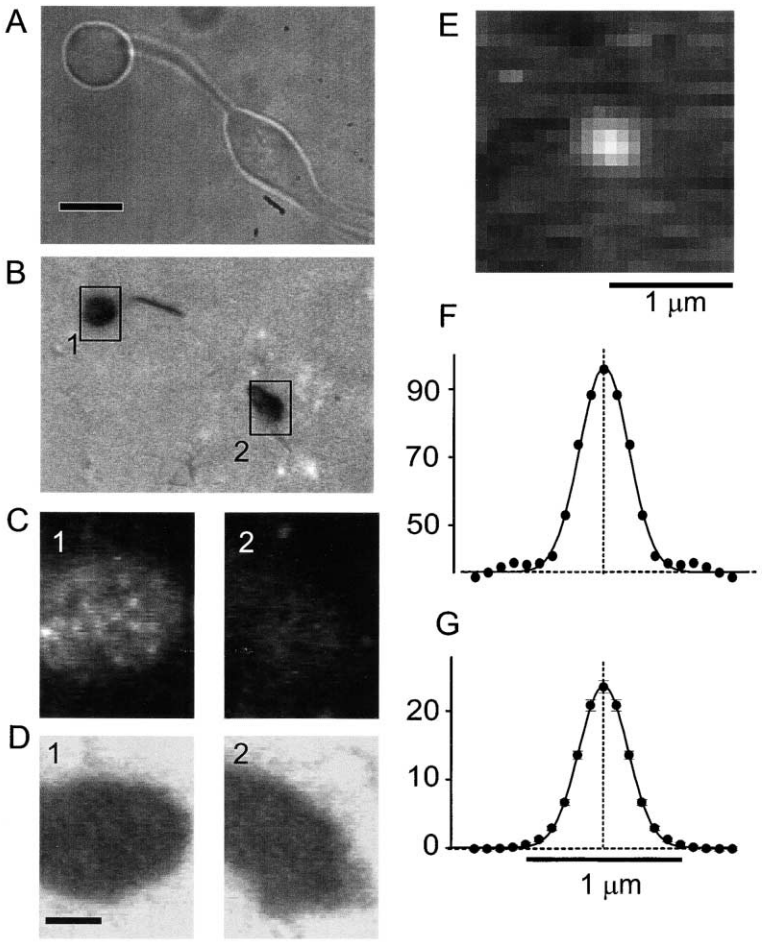

Figure 1. Imaging Single Synaptic Vesicles

(A) Brightfield image of a bipolar cell showing the terminal (upper left) connected via a short axon to the soma (lower right). Microscope focused at the center of the terminal. (B) Same cell with reflection interference contrast (IRC, for details see Steyer et al., 1997) and focused on the glass-cell interface. Regions of the cell adhering tightly to the coverslips are dark; we have estimated that regions significantly darker than background have a distance <80 nm from the coverslip (J.A.S., unpublished data). (C) Two small regions imaged by evanescent field fluorescence after staining with FM1-43. They are the same as marked in (B). (D) Regions in (C) re-imaged with IRC. (E) A small square (2.125 × 2.125 μm) excised from a larger image similar to (C) but from a different cell. It shows a vesicle that was visible for 167 ms near the plasma membrane and then retreated into the cytosol. (F) Radial sweep of the image in (E), calculated as described in the text and in Experimental Procedures. Continuous line, best fit of Gaussian function plus a constant (dashed). (G) Radial sweeps from 19 visiting vesicles as in (F) were averaged and the pixel value at 1 μm distance from the center was subtracted as background. Continuous line, Gaussian function adjusted for best fit with $\sigma = 224$ nm in Equation 1, and a full width at half maximum of 382 nm. These values are similar to measurements of FM1-43 coated 30 nm diameter beads ($\sigma = 217$ nm and full width at half maximum of 362 nm). Calibration bar in (A) is 10 μm and applies also to (B). Bar in (D) (2 μm) applies also to (C).

styryl dyes could escape from vesicles in milliseconds or less (Ryan, 2001) by diffusing in the plane of the lipid lining the pore. Indeed, exocytic fusion pores in mast cells allow membrane flux once they have dilated (Monck et al., 1990). But before dilating, fusion pores are sparingly permeable or impermeable to lipid when fusion is mediated by *Influenza* hemagglutinin (HA), a protein that fuses viral envelopes to host cells. The finding implies that HA pores are at first not lined with continuous coat of lipid (Tse et al., 1993; Chernomordik et al., 1998). Moreover, it has been suggested that fusion of yeast vacuoles begins with a proteinaceous fusion pore (Peters et al., 2001). An absence of lipid exchange in synaptic vesicles would suggest that they, too, form partly proteinaceous fusion pores.

While the results with styryl dyes are important both for the synaptic vesicle cycle and for the mechanism of membrane fusion, one may question whether they really must be interpreted as representing dye retention by synaptic vesicles (Ryan, 2001). Hence it seemed important to test whether dye retention can be seen at the level of single vesicles. This is possible when giant terminals of retinal bipolar neurons are imaged under evanescent field (EF) illumination (Zenisek et al., 2000). While conventional fluorescence microscopies have reported exocytosis as a decline in fluorescence occurring when whole terminals lose styryl dyes into the perfusion fluid, EF microscopy revealed an earlier signal of exocytosis, namely the spread of FM1-43 over the plasma membrane after it was released from individual vesicles. Our previous paper did not exclude that a portion of dye was retained due to kiss-and-run. Here we tested this point and find that most or all vesicles discharged their dye completely. At the level of single vesicles, therefore, the tracking of exocytosis with styryl dyes does not support the idea that incomplete exocytosis is a frequent event in retinal bipolar cells. In addition, we show how the escape of FM1-43 from single vesicles may be tracked independently of its spread over the plasma membrane, and explore it under conditions where brief voltage pulses stimulated synchronous and precisely timed exocytosis (Mennerick and Matthews, 1996). We find that FM1-43 leaves vesicles with a delay that is measurable but brief. Even if the fusion pore of synaptic vesicles is initially lipid impermeable, it remains so for at most a few milliseconds.

Results

Imaging Single Synaptic Vesicles

Figure 1A shows a goldfish bipolar neuron with its cell body (lower right), short axon, and giant synaptic terminal (upper left). The neuron had been plated on a glass coverslip to which it adhered tightly in small regions

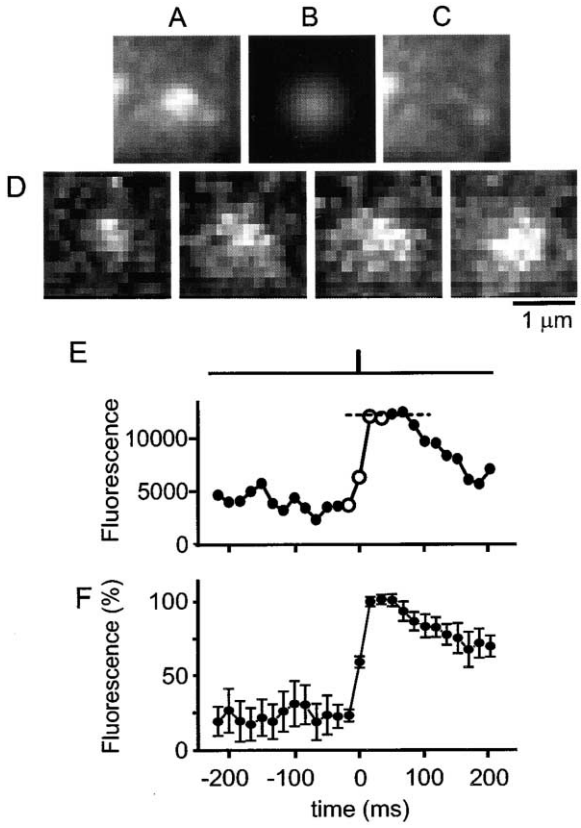

Figure 2. Exocytosis Causes an Increase in Brightness

(A) Average of five consecutive video half frames from a vesicle immediately before a voltage pulse. (B) Gaussian function that, when added to an inclined plane, provided the best least-squares fit to the vesicle in the center of (A). (C) Difference (A) − (B) is used as the local background of the vesicle. (D) Four successive video half frames after subtraction of the background image in (C); the first was taken immediately before, the others after the end of a voltage pulse that triggered exocytosis. (E) Upper, 6 ms voltage pulse to stimulate exocytosis. Lower, fluorescence against time, with the origin defined by the voltage pulse as explained in the legend of Figure 4. Each symbol represents the light summed over an entire square as in (D); open circles from the images in (D). Dashed line, average from the three video half frames immediately following the end of the voltage pulse. Because the voltage pulse was brief, we ignored here a possible increase in background fluorescence due to previous fusion events elsewhere in the cell (Zenisek et al., 2000). (F) Results from six events as in (E) (four cells) were normalized to the average of the first three values following the voltage pulse. They were then averaged together.

visualized in Figure 1B by interference reflection contrast (IRC). In IRC images, regions of the cell in close contact with the coverslip appear black (Gingell and Todd, 1979); one such region appeared beneath each, the soma, a small stretch of axon, and the terminal. Each terminal contains nearly a million synaptic vesicles (von Gersdorff et al., 1996). A small fraction of them (1%–2%, Rouze and Schwartz, 1998) were stained by briefly exposing a single cell to the fluorescent lipid FM1-43 while the cell was stimulated to undergo exo- and endocytosis. After a 0.5 to 1 hr wash in dye-free solution, the cell was ready for fluorescence microscopy. Fluorescence was excited by evanescent field illumination, which selectively illuminates an ~100 nm thin layer of cytosol adjacent to the plasma membrane in places where the cell adheres tightly to the cover glass. Figure 1C shows two such regions, one beneath the terminal (C1) and the other beneath the soma (C2). Single organelles close to the plasma membrane appear as small fluorescent spots in the terminal but not in the soma, even though reimaging by IRC (Figures 1D1 and 1D2) showed that the soma was as dark, and hence adhered as tightly, as the terminal. The selective presence of the organelles in the terminal is consistent with them being synaptic vesicles. Earlier findings support this idea (Zenisek et al., 2000).

For later analysis, it was important to characterize the image of a single vesicle with some precision. By staining only a small fraction of all synaptic vesicles, we hoped to create conditions where the fluorescent spots representing single vesicles are well separated from their stained neighbors. This strategy can fail near the synaptic ribbons that cluster vesicles beneath the plasma membrane (von Gersdorff et al., 1996). Fortunately, the plasma membrane also continuously entertains brief visits by synaptic vesicles that appear in the evanescent field and, after some 200 ms, return into the cytosol. Since such visits occur randomly over the entire footprint (D.Z. and D. Long, unpublished data), the overwhelming majority do not occur at active zones and provide our best chance of observing vesicles well separated from stained neighbors. Figure 1E shows a small square excised from a larger image (not shown) of a cell with exceptionally low background. A fluorescent spot representing a visitor appears in the center. The center was located by adjusting the amplitude, width, and position of a two-dimensional Gaussian function to provide the best least-squares fit. We calculated a "radial sweep" (see Experimental Procedures) to plot fluorescence against distance from the center (Figure 1F). The radial sweep could be fitted well by the sum of a one-dimensional Gaussian function and a constant. Figure 1G averages radial sweeps from 19 similar vesicles and represents our estimate of our microscope's point spread function for objects within the terminal. It, too, is well fitted by a Gaussian function with a full width at half maximum of 382 nm. The value is similar to that for an FM1-43 coated 30 nm bead (362 nm).

Exocytosis Increases Fluorescence

In an earlier paper, we found that exocytosis causes the fluorescence of FM1-43 from single vesicles to increase and spread over the plasma membrane (Zenisek et al., 2000). Both effects occurred in fractions of a second and preceded the much slower de-staining of plasma membrane seen if one monitors the plasma membrane fluorescence for longer times (D.Z., unpublished data). While showing that the spread of dye happens rapidly once it gets underway, these observations were unsatisfactory for our purpose for two reasons. First, the time of exocytosis was not accurately known because voltage pulses and image capture were not precisely time-locked, and because exocytic events happened stochastically throughout the 0.5–1 s voltage pulses applied to stimulate vigorous exocytosis. Second, FM1-43 must first escape from vesicles before it can spread beyond

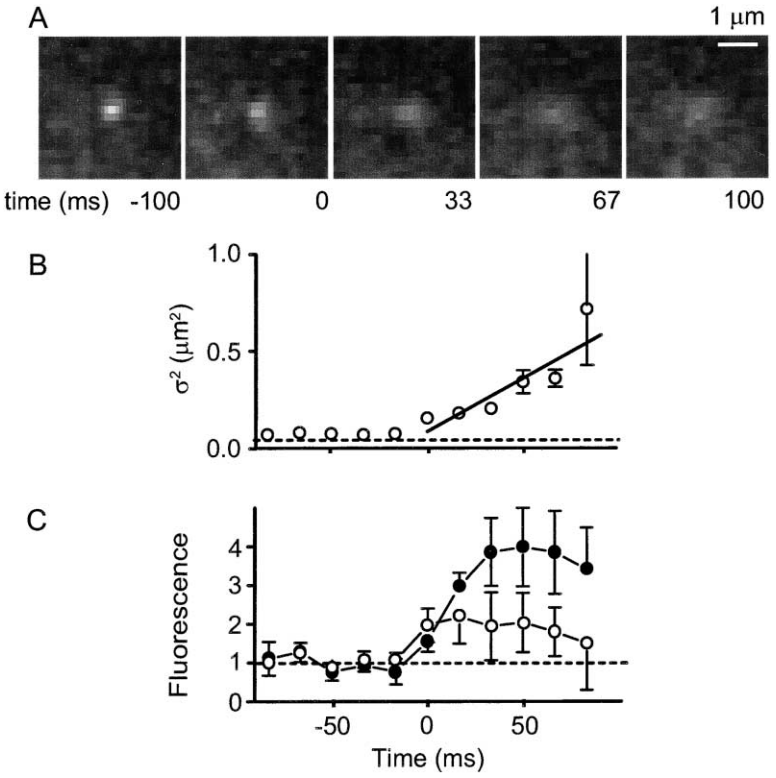

Figure 3. Effect of Polarization

(A) Images from a fusion event stimulated by a 0.5 s voltage pulse. Illumination with s-polarized evanescent light. With such long voltage pulses, fusion occurs throughout and the pulse is not a reliable time reference. Instead, here the timing is relative to the first frame where fluorescence was seen to spread. (B) From images as in (A), with a background image subtracted as in Figure 2D. For each half frame, radial sweeps measured the fluorescence as a function of distance from the vesicle's center as in Figure 1. The radial sweeps were averaged for each time point, and Gaussian curves were fitted to the result to determine the width, σ. Error bars represent the goodness of fit. Continuous line is from Figure 5D where it represents the best fit to data with p-polarized light. Dashed line indicates width of vesicle in Figure 1C. (C) Open symbols, analysis as in Figure 2E on the four vesicles under s-polarized light as in (A). Values are given relative to the average fluorescence 50 to 83 ms before fusion (dotted line). Filled symbols, as in (C) but from three vesicles from the same cell illuminated with p-polarized light. The two curves reach maxima at different times because the larger increase in brightness causes fusion to be detected earlier under p-polarized light.

the circle defined by the point spread function of the microscope. Hence dye spread, though much faster than de-staining of the entire terminal, will lag dye release.

Cells were stimulated with a precisely timed 6 ms long voltage pulse designed to cause exocytosis of only the most readily releasable vesicles (Mennerick and Matthews, 1996). This weak stimulus frequently failed to release a stained vesicle, but what release did occur is expected to be synchronous to within the few milliseconds required to empty the small pool of rapidly releasable vesicles (Mennerick and Matthews, 1996; Neves and Lagnado, 1999). Figure 2A shows a portion of a typical cell with a fluorescent vesicle in the center. The dimmer spots probably represent other synaptic vesicles at greater distance from the plasma membrane. As before (Zenisek et al., 2000), we suppressed the background and the images of other vesicles by fitting the square region in Figure 2A with an inclined plane plus a two-dimensional Gaussian function (Figure 2B). After the Gaussian function was subtracted, the vesicle in the center was no longer seen (Figure 2C). The remainder is a background image that can be subtracted from subsequent images in the same video clip. Figure 2D shows background-subtracted images taken immediately before and at various times after the voltage pulse. Fluorescence spread as the vesicle underwent exocytosis and the FM1-43 was released. The dye must have spread in the plasma membrane rather than the external medium since FM1-43 does not fluoresce in aqueous solution. The fluorescence of the dye originally in the vesicle may be tracked by summing the light in each image and plotting the results against time (Figures 2E and 2F). As before (Zenisek et al., 2000), fluorescence abruptly rose 3- to 4-fold upon exocytosis and then declined as FM1-43 spread beyond the region examined.

The Fluorescence Increase Tracks Escape of Dye from Vesicles

With more conventional methods of fluorescence microscopy, FM1-43 does not brighten on exocytosis because the fluorescence of FM1-43 is insensitive to changes experienced by the vesicle during exocytosis, such as changes in pH (Betz et al., 1996; A. Migala and W.A., unpublished data), the membrane voltage (Smith and Betz, 1996; Neves and Lagnado, 1999), or the dye concentration in the membrane (Rouze and Schwartz, 1998). Under evanescent field illumination, however, brightening may occur for two reasons. First, exocytosis inevitably brings released material closer to the glass coverslip where an evanescent field excites it more efficiently. To estimate the effect, we recall that the evanescent field declines exponentially with distance from the coverslip, falling to 37% within 43 nm (see Experimental Procedures). If a vesicle of 15 nm radius is held 3 nm from the plasma membrane, the average distance of an FM1-43 molecule from the outer leaflet of the 2.5 nm thick plasma membrane hydrocarbon layer is $15 + 3 + 2.5 = 20.5$ nm. A dye molecule moving 20.5 nm closer to the glass/water interface will be illuminated, and fluoresce, 1.6 times more intensely.

Second, as with any lipid, the orientation of FM1-43 in a planar membrane is likely to be fairly uniform. Hence light polarized perpendicularly to the plasma membrane may be more (or less) favorable for excitation than light

polarized parallel to it. In contrast, for randomly oriented molecules in bulk solvent, polarization will not matter. This should apply also to FM1-43 molecules in a spherical vesicle, where they would point with equal frequency in all directions even if their orientation remains perpendicular to the bilayer.

Light polarized perpendicular to a glass coverslip is difficult to achieve with conventional methods of illumination, but is readily obtained in an evanescent field if the beam suffering total internal reflection is p-polarized (see Experimental Procedures). Indeed, when erythrocyte plasma membrane was stained with di-I, another fluorescent lipid, fluorescence was polarization dependent, being 5-fold less when the evanescent field was generated with a p-polarized beam than with a beam polarized at right angles (s-polarized). By contrast, fluorescence of a water-soluble dye was independent of polarization (Sund et al., 1999). A related result was obtained here with FM1-43. A synaptic terminal was ruptured by stepping the membrane potential to +150 mV, causing its vesicles to spill onto the coverslip and then adhere. Fluorescence from individual vesicles was measured after background subtraction as in Figures 2A–2C (not shown). Next, the plasma membrane of an intact terminal was stained in the presence of low external [Ca^{2+}] where exocytosis does not take place and vesicles do not stain. When we compared fluorescence with p- and s-polarized light, plasma membrane fluorescence depended twice stronger on polarization than vesicle fluorescence, qualitatively as with di-I. Unlike with di-I, however, p- was more effective than s-polarized light in exciting plasma membrane fluorescence. The difference between the dyes presumably reflects the different orientations of their chromophores in the plane of the membrane.

To test whether the increased brightness upon exocytosis depends on polarization, terminals were stimulated while the beam was s-polarized, and then again with a p-polarized beam. Recordings with the two polarizations alternated. Figure 3A shows an exocytic event observed with s-polarized light. Fluorescence still spread but its increase was less. This and similar experiments were analyzed as in Figure 3B and averaged. The spread in fluorescence occurred independently of polarization but the increase in brightness was more than 2-fold less with s-polarized light (Figure 3C). Evidently, most of the brightness increase was a polarization effect occurring as dye moved from a sphere (the vesicle) into a planar structure (the plasma membrane).

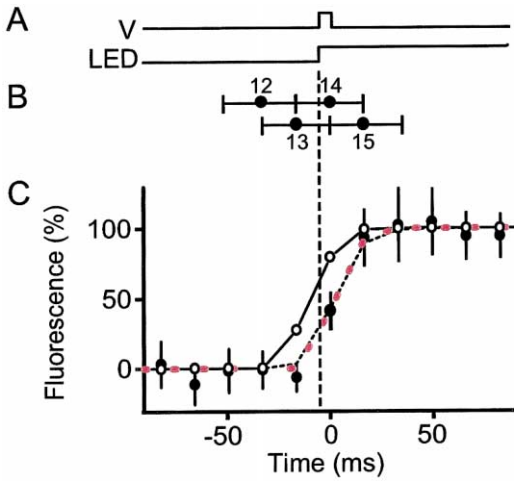

Figure 4. Escape of Dye after a Brief Stimulus

(A) A 6 ms voltage pulse applied to the cell (V) and a voltage step applied to a light-emitting diode (LED) in parallel experiments. Pulse and step started 8 ms before the end of light collection for the 13th half frame. (B) Light collection by a video camera. Video cameras records 30 full frames/s, each superimposing two half frames, one containing the odd- and the other the even-numbered horizontal rows of pixels. To improve time resolution, individual half frames were recovered so that 60 half frames/s alternated in showing odd-numbered or even-numbered horizontal pixel rows. Each half frame collects light over a 33.3 ms interval, so that the collection intervals for successive half frames overlap by 16.7 ms. The schematic drawing shows the intervals over which the camera collected light for the half frames labeled 12 through 15, with their midpoints shown as filled circles. The midpoint of the collection interval for half frame 14 occurred 0.7 ms before the time origin. If an LED is lit by a voltage step starting 8 ms before the end of the 13th half frame, we expect the 12th half frame to receive no light. The 13th is lit for the last 8 of its 33.33 ms, hence the camera is expected to read 24% of the value measured under continuous illumination. The 14th half frame is lit for the last 24.7 of its 33.3 ms, and should record 74%. The 15th and all following half frames are lit continuously and record 100%. (C) Light collected as percentage of maximum, with data points placed at the centers of the light collection intervals. Open circles, recording of the LED output in response to a voltage step. The data fit well with the prediction made in (B). Filled circles, data in Figure 2F normalized so that the average of the first five half frames read 0, and the maximum 100%. Black and red dotted lines are model calculations that account for the distortions introduced by the timing of light collection, and for the delay between voltage pulse and exocytosis (see Discussion). The red dotted line assumes that the vesicle releases all its dye at once. The best fit required a delay of 10.7 ms after the beginning of the voltage pulse. The black dotted line assumed that release starts with a fixed delay of 4.5 ms, and proceeds exponentially until the vesicle is empty. A time constant of 6.1 ms provided the best fit.

Delayed Release of Dye

We conclude that exocytosis causes FM1-43 to brighten for two reasons: increased proximity to the coverslip and, more importantly, the more favorable orientation of dye in the plasma membrane. Both result from the release of dye into the plasma membrane, and occur independently of the subsequent spread of the dye. Hence the fluorescence rise in Figure 2E can be used to determine how soon and how rapidly synaptic vesicles release dye. Clearly dye release was fast. If it were instant, how rapidly would the camera report the fluorescence increase? This is tested in Figure 4C where a light-emitting diode (LED) was lit by a maintained voltage step starting at the same time as a 6 ms voltage pulse to the terminal (Figure 4A). Even though the LED lit instantly, the camera spread the increase in light over some 50 ms (open symbols in Figure 4C) and made it seem to begin before the voltage pulse. The finding is explained in Figure 4 (legend).

The LED recording may be compared with the data of Figure 2F replotted on an expanded timescale. The rise in FM1-43 fluorescence shows a delay whose magnitude is best appreciated in a model calculation. As-

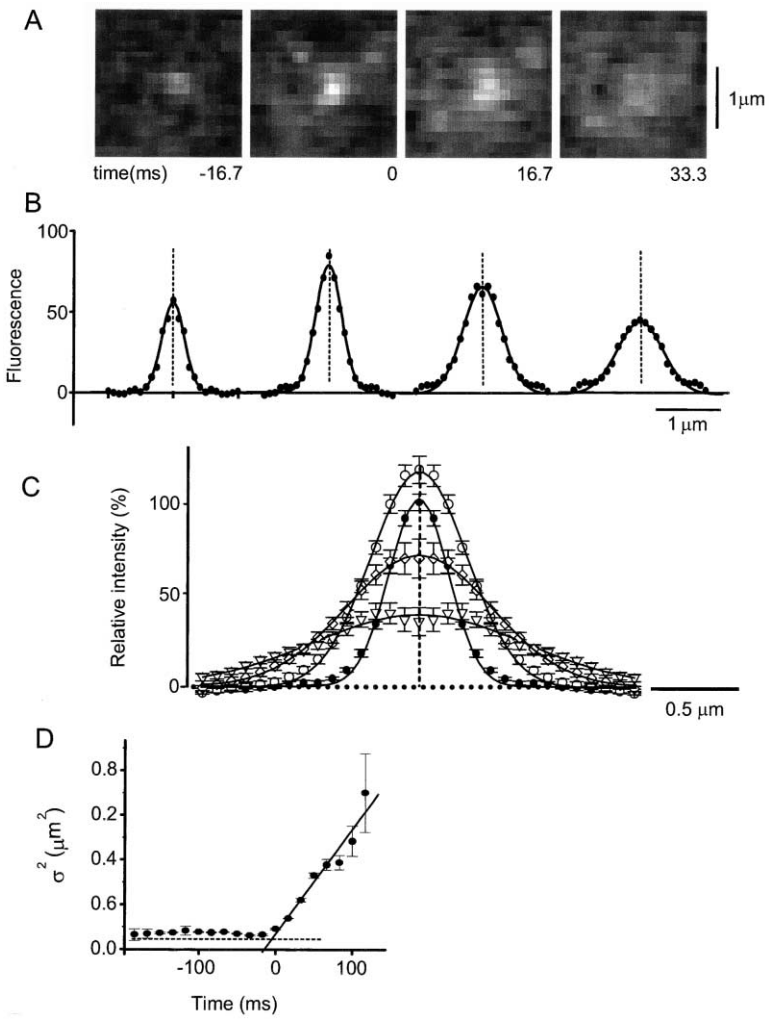

Figure 5. Diffusion of FM1-43 following Exocytosis

(A) Consecutive half frames showing exocytosis during a 0.5 s pulse. (B) Radial sweeps of the images in (A) calculated as described in Figure 1 and in Experimental Procedures. Except for the peak, which relies on a single pixel only, line scans are well described by Gaussian functions. The asymptote of the Gaussian function defines the origin for the ordinate. (C) Average fluorescence profiles at selected times relative to fusion (filled circles, −17 ms; open circles, 17 ms; diamonds, 50 ms; and triangles, 133 ms). Cells stimulated with 0.5 s pulses. We selected 15 vesicles that had no other fusion events in their neighborhood and were located >0.5 μm from the cell's edge. Video sequences as in (A) were excised and aligned in time to the first half frame showing fusion. In this figure, fusion was determined to have occurred when fluorescence was first seen to both increase and spread. In each of the 15 sequences, radial sweeps were calculated as in (B), and scaled relative to the mean peak intensity over the last 10 half frames before fusion. The results were then averaged. The lower amplitude of the curve before fusion (filled circles) results from the overall fluorescence increase on exocytosis. Continuous curves are best fits of Gaussian functions. (D) Timecourse of σ^2, the square of the width of the Gaussian curves. Error bars, standard errors reflecting the goodness of fit. The line is a best fit to the points at $t > 0$ ms, weighted inversely by the square of their error bars. Its slope corresponds to a diffusion coefficient of 1.17 μm²/s. Dotted horizontal line, σ^2 for vesicle profile of Figure 1C.

sume that the release of dye, once underway, occurs instantly on the timescale of Figure 4B. This would happen if the exocytic fusion pore of the vesicle were lipid impermeable at first but, after a delay, dilated explosively and released all dye at once. The data are best accounted for if the release occurs 11 ms after the start of the voltage pulse (red dotted line in Figure 4C). Alternatively, it may be supposed that a lipid-permeable fusion pore opens 4.5 ms after the beginning of the voltage pulse (see Discussion) and empties the vesicle of dye along an exponential function. The data are fit best if the time constant is 6.1 ms (black dotted line).

Diffusion of FM1-43 in the Plane of the Plasma Membrane

To explain why styryl dyes fail to enter or leave synaptic vesicles, it was suggested that FM1-43 may not diffuse freely in membranes of a synaptic terminal (Ryan, 2001). We determined the diffusion coefficient of FM1-43 by treating the spread of dye out of a fusing vesicle as diffusion from a point source in a plane (Crank, 1970):

$$F = A_1 \exp[-r^2/\sigma_1^2] \quad (1)$$

where the local fluorescence F is the concentration of the diffusing substance as a function of time, t. A_1 is the peak amplitude, r is the distance from the point source, and the width parameter σ_1 is equal to $(4Dt)^{1/2}$ where D is the diffusion coefficient. When our imaging system records the spread of dye, it blurs a synaptic vesicle or a concentration profile by convolving it with the point spread function of our imaging system. Inasmuch as the point spread function determined in Figure 1 approximates a Gaussian function (width parameter 0.055 μm²), the result is another Gaussian with width parameter $\sigma^2 = (4Dt + 0.055\ \mu m^2)$. When, therefore, Gaussian functions are fitted to fluorescence images, their width parameter should increase linearly with time, the slope of the line being 4D (Schmoranzer et al., 2000).

Figure 5A shows images of a fusing vesicle as in Figure 2. Radial sweeps were calculated for each image and fitted by Gaussian functions (Figure 5B). Figure 5C averages radial sweeps from this and similar experiments and shows Gaussian curves providing the best fit. Their width parameter σ^2 is plotted against time in Figure 5D. The spread of dye can be followed over >100 ms after fusion. The points are well fitted by a straight line corresponding to a diffusion coefficient of 1.2 μm²/s. This is similar to values for Di-I in red blood cells (1.0 μm²/s;

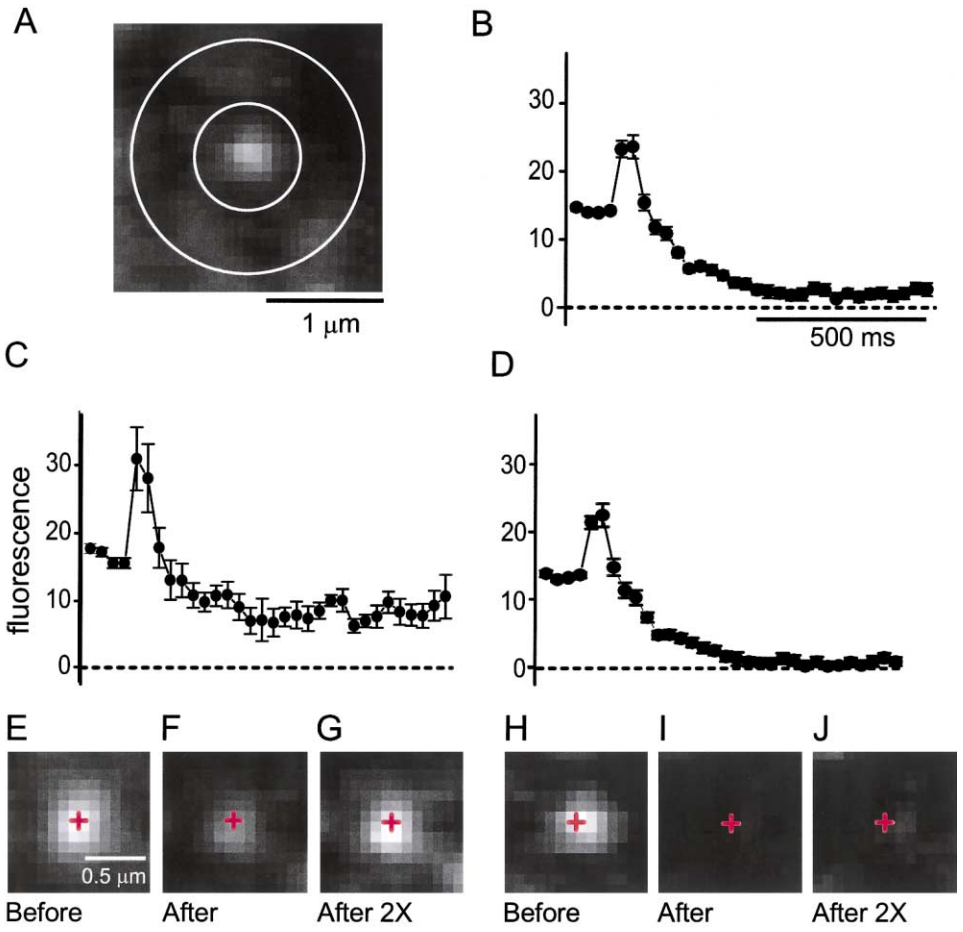

Figure 6. Fluorescence Remains near Some Fusion Sites

(A) Vesicle surrounded by two concentric circles (0.935 μm and 2.125 μm diameter) defining a circle and annulus for the measurement of radial gradients in fluorescence. (B) Fluorescence intensity difference (circle minus annulus) as a function of time. The brief, spike-like fluorescence increase marks fusion and defines the time origin; it is sharper than in Figure 2E because the circle was smaller so that dye diffused out of it more quickly. Average of 41 fusion events in four cells aligned to the instant of fusion. To qualify for selection, events occurred >0.5 μm from the cell's edge. For each event, the initial (pre-fusion) value was determined as the mean of the last four values before fusion. The post-fusion value was the mean of frames 15–24 after fusion, corresponding to 500–867 ms after fusion. The curves were first normalized to their pre-fusion values, then averaged and finally multiplied by the average pre-fusion value. (C) A subset of seven events drawn from the data set in (B) plotted separately (subset 1). They were selected to have post-fusion values of >40% of the initial value. Results for the remaining vesicles plotted in (D). (E– G) Images from a member of subset 1. Images are averages of the last four frames before fusion (E) and the 22nd to 25th after fusion (F). (G) is (F) reprinted at twice the brightness. (H–J) As in (E)–(G) but for one of 8 outliers in the data set of (B). Outliers are defined as occurring at distances of >500 nm from the nearest site of any other fusion. Full frames throughout. Cells stimulated by single 0.5 or 1.0 s pulses, or by trains of 30 ms pulses given at 4 Hz.

Bloom and Webb, 1983) and fibroblasts (1.0–1.4 $\mu m^2/s$; Jacobson et al., 1981). Evidently, FM1-43 in the terminal membrane diffuses no less freely than lipids in other cell membranes.

Do Vesicles Retain Dye after Exocytosis?

Earlier work (Zenisek et al., 2000) showed that exocytosis causes some FM1-43 to diffuse out of the vesicle and into the plasma membrane. However, it remained possible that the fusion pore closed before all FM1-43 could escape, thus trapping some dye within the vesicle (Klingauf et al., 1998; Pyle et al., 2000). To test this point, we placed a small circle and an annulus around the vesicle, with the small circle just large enough to accommodate the image of the vesicle (Figure 6A). The difference in fluorescence intensities between the two regions was plotted against time while the vesicle underwent exocytosis (Figure 6B). The difference first increased as in Figure 2, then declined; it was expected to disappear as dye equilibrates. However, even 700 ms after exocytosis, there remained a difference of 12% ± 5% of the initial value, possibly consistent with the idea that at least some vesicles fail to discharge all dye.

Closer inspection showed that this effect was due to a subset of one sixth of the vesicles retaining 51% ± 2% of their initial fluorescence difference (subset 1, plotted separately in Figure 6C). All were contained in small, discrete "active zones" of exocytosis (Zenisek et al., 2000), defined here as any region within 300 nm of at least one other fusion event in the same cell. For the remaining 34 vesicles, our data indicate complete equilibration (to 5% ± 5% of initial difference, Figure 6D).

Some resided in active zones while others populated the remainder of the cell membrane as solitary "outliers."

To explore why dye remained at the fusion site in Figure 6C, Figures 6E–6G show images from a sample event in subset 1, one image just before and two well after fusion. As a control, images from the fusion of an outlier are also shown (Figures 6H–6J). Before fusion, vesicles in subset 1 appeared slightly larger than outliers, and after fusion, a dim fluorescent spot remained slightly off center. Fusion of outliers resulted in darkness.

It seemed possible that the vesicle in Figures 6E–6G disconnected from the plasma membrane before all its dye could leave, and later moved off center where it remained visible as a dim spot. To explore this idea, we obtained for each event in subset 1 a pair of images as in Figures 6E and 6F. Images before fusion were centered and superimposed to form averages; then radial sweeps were made (Figure 7A, left). Radial sweeps of images well after fusion were also made (Figure 7A, right). We proceeded similarly with outliers (Figure 7C). Results for outliers were unremarkable. Before fusion, there was a sharp peak as expected from a solitary single vesicle and fusion caused it to disappear, as in Figures 6H–6J. For subset 1, however, the fluorescence profile before fusion could not be explained by a single vesicle. Its shoulders required adding a broad Gaussian function (dashed). When analyzed as in Figure 6A, the broad Gaussian contributed 55% of the pre-fusion fluorescence difference between a circle and a concentric annulus. Interestingly, the same broad Gaussian function accounts also for more than 90% of the difference remaining after fusion. This suggests that most of the fluorescence after fusion was already present before, and that much of it arose outside the fusing vesicle. This portion cannot be due to incomplete discharge. To account for all fluorescence after fusion, however, one must add a portion of the profile in Figure 1G that is 0.24 times as large as that required before fusion. We conclude that about a quarter of the dye may have remained in 7 of 41 vesicles. If FM1-43 leaves a vesicle with a time constant of 6 ms (Figure 4), then the fusion pores in subset 1 remained open for 9 ms. In the remainder of vesicles, equilibration and hence discharge of dye were essentially complete. The fusion pore must have stayed open for $>$20 ms and may have never closed.

What could cause the larger and more blurred image of the vesicle in Figure 6E, and the corresponding residual light represented by the broad Gaussian curve in Figure 7A? A partial explanation is based on the finding that such events occur only at active zones where synaptic ribbons are expected to concentrate vesicles in submembrane clusters (Figure 7B). Where a ribbon holds one or more additional stained vesicles, these will appear dim inasmuch as they are held some distance from the membrane. If not discretely resolved, they will tend to make fluorescent spots look larger, and after fusion they will remain as dim spots that may be slightly off center, as in Figures 6E and 6F. The broad profiles in Figures 7A and 7B could thus result from the superposition of dim vesicles held slightly off center. Broad profiles are not expected outside active zones, nor at active zones that hold no stained vesicles other than the one

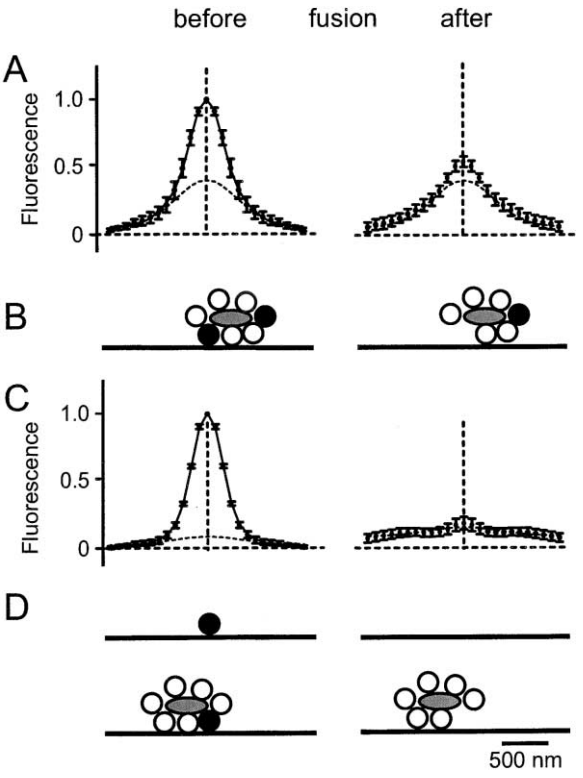

Figure 7. Some Residual Fluorescence Is Unrelated to Vesicle Fusion

(A and C) Average of radial sweeps immediately before and 500 to 833 ms after fusion, compiled from vesicles with significant residual fluorescence (A, subset 1) and from outliers (C). *Before*, for each event the last four full frames before fusion were averaged and a radial sweep calculated. The value around a perimeter at 14 pixels (1.2 μm) distance from the center was subtracted as background, and the result was normalized to the value at the center. Results from seven events were averaged. Continuous line adds a fraction of the radial sweep of Figure 1G (0.62), a Gaussian function (amplitude 0.34), and a small offset (0.04). These three parameters as well as the width of the Gaussian were adjusted to provide the best fit. The dashed line plots the Gaussian function plus offset separately. *After*, similar to *before* but frames 15 to 24 after fusion were averaged for each event prior to calculating a radial sweep. The calculation of the sweep used the same center position as *before*, as well as the same values for background subtraction and normalization. Continuous line, sum of the Gaussian function and offset *before* (dashed) plus a fraction (0.146) of the amplitude in Figure 1G, adjusted for best fit. (B) Possible origin of the residual fluorescence from labeled vesicles held on a synaptic ribbon at varying distances, both vertically from the plasma membrane and laterally from the fusion site. Because (A) is an average, vesicles at the different positions are not discretely visible and instead superimpose to cause a blurred image represented in (A) by a broad Gaussian function. After fusion, only the vesicle at the fusion site is lost, while the broad Gaussian remains as a major source of residual brightness. (C) As in (A) for 11 outliers. *Before*, the profile in Figure 1G was scaled to an amplitude of 0.92, the amplitude of the Gaussian was 0.07, and of the offset 0.02. *After*, data processed as in (A). A dashed line showing the Gaussian *before* after increasing the offset is buried beneath the data points. (D) Little or no fluorescence remains when only the fusing vesicle is visible, either as an outlier or as the only stained vesicle on a ribbon. Since each ribbon has of the order of 110 vesicles (von Gersdorff et al., 1996) and only 1%–2% of all vesicles are stained, many ribbons will hold only one stained vesicle.

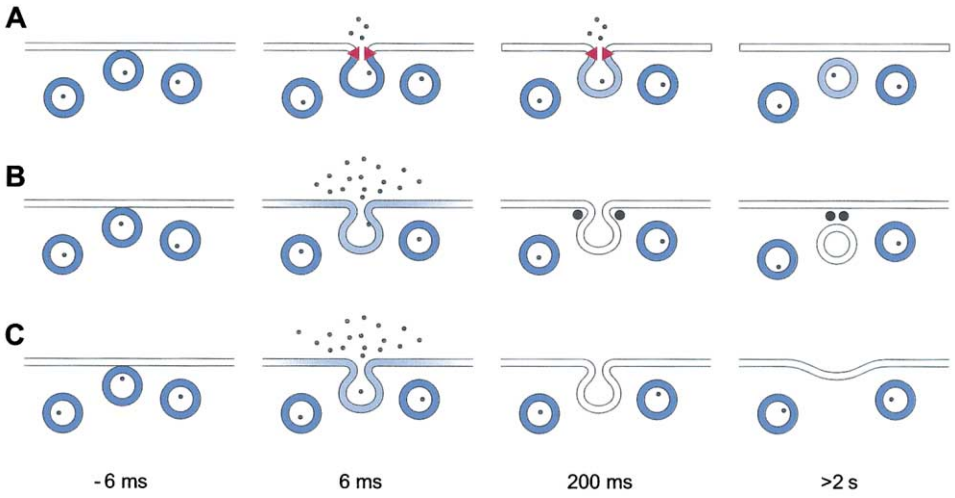

Figure 8. Three Fates of Synaptic Vesicle after Exocytosis

Incomplete (A and B) and complete fusions (C). (A) A lipid-impermeable fusion pore prevents escape via the lipid bilayer, and dye must desorb from the vesicle membrane before it escapes. Dye remains in the vesicle when the fusion pore closes again. (B) Dye rapidly leaves the vesicle by diffusion in the lipid bilayer, and only later desorbs from the plasma membrane. Later, the fusion pore closes again, possibly through the action of fission-mediating proteins assembling at the exocytic site (large black dots). (C) Dye escapes as in (B), but the vesicle flattens into the plasma membrane. Times given relative to the moment of fusion. Small dots represent dye molecules in solution. Dissolved dye molecules in vesicles are rare. At 5 μM concentration, there would be on average 0.04 FM1-43 molecules in a vesicle.

that fuses (Figure 7D). Indeed, the contribution of a broad Gaussian is undetectable with outliers.

Disappearance of Vesicles without FM1-43 Release

In a cell line derived from pancreatic β cells, dense core granules occasionally discharge their soluble contents but close their fusion pore before granule membrane proteins escape. The granule cavity thus retrieved then detaches from the membrane and moves into the cytosol (Tsuboi et al., 2000). Some synaptic vesicles may behave in an analogous fashion, release transmitter but no dye (Stevens and Williams, 2000) and then depart into the cytosol. In our assay, such events would present as resident vesicles that leave the plasma membrane without releasing dye. Only rarely (4 of 50) did resident vesicles in a stimulated cell disappear into the cell without spilling dye into the plasma membrane. At active zones, none of 30 resident vesicles disappeared without discharging dye.

Discussion

Some neurobiologists have long held that synaptic vesicles may release transmitter through transient fusion pores, and then disconnect from the plasma membrane without flattening into it (Torri-Tarelli et al., 1985) nor losing their membrane proteins (Valtorta et al., 1990). This view was recently revived under the name kiss-and-run exocytosis (Fesce et al., 1994), defined as the "direct reversal of the exocytic process without intermixing (of vesicle membrane components) with the presynaptic membrane" (Valtorta et al., 2001). The term included (Valtorta et al., 2001) the concept of "rapid endocytosis/retrieval" followed by "re-use" of the vesicle (Pyle et al., 2000). Kiss-and-run was based on findings suggesting that synaptic terminals fail to incorporate (Stevens and Williams, 2000; Verstreken et al., 2002) and/or release styryl dyes such as FM2-10 and FM1-43 while releasing transmitter (Henkel and Betz, 1995; Klingauf et al., 1998; Pyle et al., 2000; Stevens and Williams, 2000). The conclusion reached, namely that synaptic vesicles close their pore before dye can enter or leave them, may be taken as the current operational definition of kiss-and-run at synapses.

Lipidic dyes such as FM2-10 and FM1-43 can leave a synaptic vesicle via two routes. The first requires that dye molecules desorb from the vesicle membrane into the lumen and then diffuse within the aqueous phase out of the vesicle (Figure 8A). A preferred use of this aqueous route is suggested by the finding that FM2-10-stained terminals de-stain more readily than terminals stained with the more slowly desorbing dye FM1-43 (Klingauf et al., 1998; Pyle et al., 2000). The second route exists in addition to the first. Instead of desorbing, dye molecules diffuse along lipid bilayer that may line the neck of the fusion pore (Figure 8B). This lipidic route is expected to be orders of magnitude faster (Ryan, 2001) unless styryl dyes diffuse within membranes much more slowly than other lipids (a possibility excluded in Figure 5), or unless a molecular barrier (red in Figure 8A) makes the fusion pore lipid impermeable. If the lipidic route is passable, any retention of dye requires fusion pores to close within milliseconds or fractions thereof. Pore closure in $<$6 ms was envisioned by Stevens and Williams (2000) who suggested that it may represent the molecular reverse of pore opening. Similarly, fast pore closure would explain the early electron microscopic results of Torri-Tarelli et al. (1985).

The mechanism of kiss-and-run aside, must the results with styryl dyes be interpreted as dye retention by single vesicles? We examined this question in terminals of goldfish bipolar neurons where single vesicles can

be observed directly. These large terminals differ from hippocampal neurons in forming ribbon synapses and containing several 1000 times more vesicles. Nonetheless, as in hippocampal neurons, transmitter release is mediated by a small subset of synaptic vesicles comprising the rapidly releasable pool. In hippocampal neurons, this pool is thought identical to the pool of vesicles that are docked to the plasma membrane (Schikorski and Stevens, 2001), and held primarily responsible for kiss-and-run. The vesicles observed here are also clearly docked in that they are immobilized so close to the plasma membrane (within 10 nm; Zenisek et al., 2000) that they undergo exocytosis without approaching the plasma membrane any further. Moreover, the vesicle population studied here is as rapidly releasable (von Gersdorff and Matthews, 1994; Mennerick and Matthews, 1996) as that in hippocampal neurons (Stevens and Tsujimoto, 1995). Finally, the readily releasable vesicle pools are replenished as rapidly in goldfish bipolar terminals (Mennerick and Matthews, 1996; von Gersdorff and Matthews, 1997; Gomis et al., 1999) as they are in hippocampal neurons (Stevens and Tsujimoto, 1995). Therefore, the vesicle pool studied here is functionally analogous to that thought to undergo kiss-and-run in hippocampal neurons.

Surprisingly, we found little or no evidence for dye retention by single vesicles. In bipolar neurons, 90% of vesicles resident at active zones release dye during a 0.5 to 1 s stimulus (Zenisek et al., 2000), and we show here that they release essentially all of it in a fraction of a second. Our result differs from conclusions in hippocampal neurons (Pyle et al., 2000) that (1) dye retention is the specific and near uniform behavior of the vesicles comprising the rapidly releasable pool, (2) the fusion pore stays open for an entire second, and (3) a vesicle releases only one-third of its FM1-43 during that time (time constant of 2.6 s).

This striking difference may well be genuine and reflect the different morphologies of the two neurons and the different synaptic activities mediated by them. Incomplete exocytosis, kiss-and-run, and re-use seem most advantageous at synapses with few vesicles to spare, such as hippocampal synapses (Pyle et al., 2000). But these mechanisms risk that empty vesicles continue to occupy precious docking sites and undergo exocytosis before they are refilled with transmitter. In bipolar neurons with their nearly one million vesicles and their need for continuous transmitter release, the risk may not be worth taking.

Alternatively, one may question whether dye retention by whole terminals necessarily means dye retention by single vesicles. The differential de-staining of FM20-10 and FM1-43 (Klingauf et al., 1998; Pyle et al., 2000) does suggest that terminals have an endocytic mechanism fast enough to compete with the slow desorption of FM1-43 but not with that of FM2-10. But it is less clear whether the dyes desorb into the synaptic vesicle or mainly into some other space with restricted access from which synaptic vesicles bud by genuine endocytosis. In frog motor neurons, for example, the retention of FM1-43 was first attributed to synaptic vesicles (Henkel and Betz, 1995) but later found to occur in deeply invaginated cisternae that formed during stimulation (Richards et al., 2000), consistent with the original model of Heuser and Reese (1973). Moreover, other investigators have obtained different results even in hippocampal neurons. Unlike Pyle et al. (2000), Stevens and Williams (2000) found no difference between FM2-10 and FM1-43, but did find that dye retention (and hence kiss-and-run) was more pronounced when terminals were stimulated with sucrose rather than electrically. This may be partly because such differences were what their assay could detect.

While Stevens and Williams (2000) did not test for dye retention under physiological conditions, they inferred its occurrence by extrapolating a model calculation and concluded that 20% of synaptic vesicles in the readily releasable pool released transmitter without releasing dye. Such events would be missed in our assay, but they can account for no more than 10% because 90% of vesicles docked at active zones release FM1-43 during a voltage pulse (Zenisek et al., 2000).

Is the Exocytic Fusion Pore Initially Impermeable to Lipid?

FM1-43 in bipolar neurons ultimately escapes into the plasma membrane, but this does not exclude that a lipid-impermeable fusion pore initially prevents such escape. As in *Influenza* hemagglutinin-mediated membrane fusion (Tse et al., 1993; Chernomordik et al., 1998), fusion pores may be lipid impermeable when they first open, but later expand to allow lipid exchange. Indeed, the difference between hippocampal and bipolar neurons may be simply that the pore expands sooner in bipolar neurons.

To address this point, we used brief voltage pulses for precise timing of exocytosis. In addition, we were able to track the escape of dye from synaptic vesicles independently of its subsequent spread over the plasma membrane by taking advantage of the increase in FM1-43 fluorescence upon exocytosis. We identified two factors causing this effect. First, exocytosis brings dye into the plasma membrane and hence closer to the glass/cell interface where the evanescent field is stronger. Second, as dye molecules leave a sphere (the synaptic vesicle) where they point in all directions, they enter a plane (the plasma membrane) where their orientation is more uniform and where they are excited more effectively by p-polarized light.

Taking due account of the time resolution of our camera, we found that dye release lagged a brief stimulus by about 11 ms. Electrophysiologic data suggest that this is longer than the time required to trigger and execute exocytosis. In capacitance measurements, exocytosis during a short pulse such as in Figures 2 and 4 occurs during the first few milliseconds as it depletes a small pool of the most rapidly releasable vesicles with a time constant of around 1.3 ms (Mennerick and Matthews, 1996) to 2.2 ms (Neves and Lagnado, 1999). These studies did not exclude a small delay between the rise of $[Ca^{2+}]$ and the exocytosis of the first vesicles. But this delay is only 1 to 2 ms until the first sign of a capacitance increase (Heidelberger et al., 1994) and 0.8 ms until the first signs of glutamate release (von Gersdorff et al., 1998). If we allow 0.5 ms for the propagation of the voltage pulse into the terminal (Mennerick et al., 1997), a delay of 2 ms between the rise of $[Ca^{2+}]$ and

exocytosis of the first vesicles, and finally a time constant of 2 ms for the exhaustion of the most readily releasable vesicle pool, then the average vesicle opened its fusion pore within 4.5 ms of the voltage pulse. Since dye release occurred with a 11 ms delay, it must have occupied the remaining 6–7 ms. While 6 ms may not seem a long time, it is 20 times longer than the time required for transmitter release in leech neurons (time constant 260 μs; Bruns and Jahn, 1995).

The lines drawn into Figure 4C represent two models. In the first (red dotted line), the fusion pore is completely lipid impermeable for 6.5 ms but then dilates abruptly, causing all dye to be released at once and the vesicle to flatten into the cell surface. In the second model, a lipid-permeable fusion pore does not dilate but remains the main barrier to dye release. In this model, dye leaves the vesicle exponentially, and the best fit requires a time constant of 6.1 ms (Figure 4C, dashed line). Both fit the data equally well. We conclude that dye escapes from the vesicle within a few milliseconds. If the fusion pore is initially lipid impermeable, it remains so for less than 7 ms.

Complete and Incomplete Exocytosis

Figure 8 shows three current models of synaptic vesicle exocytosis. In one form of kiss-and-run (Figure 8A), the fusion pore prevents the exchange of lipid between vesicle and plasma membrane for seconds and then closes so that significant FM1-43 remains in vesicles. Similar models would apply wherever styryl dyes must desorb before they can leave the vesicle. In another form of kiss-and-run (not shown), the fusion pore closes so rapidly that no molecular barriers are needed to prevent membrane mixing. Kiss-and-run is rare or absent in bipolar cells The other two models are consistent with our results. In Figure 8B, exocytosis starts with the opening of a fusion pore that is lipid permeable from the beginning, or becomes lipid permeable within milliseconds after opening. FM1-43 escapes into the plasma membrane nearly completely within the first 20 ms. The pore closes later, possibly after recruiting dynamin or other molecules (filled circles in Figure 8B) to execute fission. Fusion pores formed by dense core granules in mast cells do allow lipid exchange after they have dilated (Monck et al., 1990) and still can close completely (Spruce et al., 1990; Monck et al., 1990; Ales et al., 1999). After fissioning, vesicles can be re-used provided they retained their membrane proteins. At least some vesicles lose the SNARE protein VAMP/synaptobrevin in hippocampal neurons (Sankaranarayanan and Ryan, 2000). Re-use may not be common in bipolar neurons, as fresh vesicles replace those lost by exocytosis within a few seconds (Zenisek et al., 2000). Figure 8C shows complete exocytosis where dye is released and where the vesicle flattens into the cell membrane to be retrieved later by clathrin-mediated endocytosis. In lamprey spinal neurons, this model is supported by increasingly detailed functional and molecular evidence (Slepnev and de Camilli, 2000).

The weight of the evidence suggests to us that kiss-and-run is rare in synaptic vesicles under normal conditions, at least in its strict definition where the exchange even of lipids is prevented or strongly hindered (Valtorta et al., 2001). It was too rare to be reliably detected in the present work on bipolar neurons. We find it hard to imagine how kiss-and-run can be definitively established other than at the level of single vesicles. This may now be possible with electrophysiologic recording (Klyachko and Jackson, 2002). Further studies will take advantage of conditions where kiss-and-run becomes prevalent. An interesting recent example is a *Drosophila* mutant where clathrin-mediated endocytosis fails through lack of the protein endophilin (Verstreken et al., 2002). In *Drosophila*, the mechanism appears to require dynamin as it fails in the *shibire* mutant (Verstreken et al., 2002). Ultimately it will be important to discover whether the mechanism is ever called upon under physiologic conditions.

Experimental Procedures

Cells, Fluorescent Staining, and Solutions

Bipolar neurons were prepared as described previously (Heidelberger and Matthews, 1992). Briefly, goldfish were killed and eyes were removed and hemisected. To remove the vitreous, eyecups were incubated for 20 min in hyaluronidase (Sigma type V; 1100 units/ml) in a solution containing (in mM): 120 NaCl, 0.5 $CaCl_2$, 2.5 KCl, 1.0 $MgCl_2$, 10 glucose, 10 HEPES (pH 7.4 with NaOH). Retinas were then removed from eyecups, cut into approximately eight pieces each, and incubated for 35 min in a solution of 35 units/ml papain (lyophilized powder; Sigma), 0.5 mg/ml cysteine, and (in mM) 120 NaCl, 0.5 $CaCl_2$, 2.5 KCl, 1.0 $MgCl_2$, 10 glucose, 10 HEPES (pH 7.4 with NaOH). After enzymatic treatment, tissue was washed in enzyme-free solution and stored at room temperature. The pieces of retina were dissociated into single cells by mechanical trituration. For staining and observation, cells were plated in recording solution containing (in mM): 120 NaCl, 2.5 $CaCl_2$, 2.5 KCl, 1.0 $MgCl_2$, 10 glucose, 10 HEPES (pH 7.4 with NaOH) on special coverslips made from high refractive index glass (n_{488} = 1.80; Plan Optik, Germany).

Bipolar cells were recognized by their large synaptic terminal and unique cell body morphology (Figure 1A). Cells were pulse-labeled with FM1-43 as described previously (Zenisek et al., 2000). A selected cell was locally superfused for 10 s with a solution containing 5 μM FM1-43 (Molecular Probes) and (in mM) 2.5 $CaCl_2$, 25 KCl, 95 NaCl, 1.0 $MgCl_2$, 10 glucose, and 10 HEPES (pH 7.4 with CsOH). This solution is expected to stimulate exocytosis. Next, the cell was washed by local superfusion for 30–60 min with a low calcium solution designed to stop exocytosis. It contained (in mM): 120 NaCl, 0.5 $CaCl_2$, 2.5 KCl, 1.0 $MgCl_2$, 10 glucose, 10 HEPES, and 1.25 mM EGTA (pH7.4 with NaOH). After the wash, the superfusion was switched to recording solution. A pipette was sealed against the cell body, and the patch of membrane beneath its tip was ruptured to gain electrical access. The cell body was voltage clamped using an EPC-9 amplifier (Heka), running Pulse (Instrutech) stimulus and acquisition software. The pipette solution contained (in mM): 120 Cs-glutamate, 4 Na_2ATP, 0.5 GTP, 4 $MgCl_2$, 10 TEA-Cl (pH 7.2 with CsOH). Exocytosis was triggered by voltage steps to 0 mV. A gravity-fed bath perfusion system perfused the entire chamber with recording solution throughout the staining period and the experiment. Means are given as ± standard error.

Imaging and Data Acquisition

Cells were viewed through an inverted microscope (Zeiss Axiovert 135) modified for through-the-objective evanescent field illumination (Axelrod, 2001; Steyer and Almers, 2001). A 488 nm wavelength beam from an argon laser (Coherent) was applied by opening and closing a shutter for 0.5–3 s long periods of observation. The beam was expanded and focused off axis onto the back focal plane of a 1.65 NA objective (Apo ×100 O HR, Olympus). After leaving the objective, light entered immersion oil of high refractive index (n_{488} = 1.80, Cargille, XX) and then a coverslip of similar refractive index glass (n_{488} = 1.80). The beam suffered total internal reflection as it struck, at a glancing angle, the interface between the glass and the solution or cell. Total internal reflection generates an evanescent

field declining exponentially with distance from the interface. The depth of penetration depends on the angle at which light strikes the glass/cell interface. To measure this angle, a hemicylinder with the same refractive index as the coverslip was decorated with a drop of high refractive index immersion oil and placed and centered on top of the objective. Light left the prism at an angle of 65.6°–68.0°. Given the refractive indices of cytosol (n = 1.37) and glass (n = 1.80) and the 65.6°–68.0° angle, the evanescent field illuminating fluorescent structures is expected to decline e-fold in 41–43 nm. Fluorescence images were intensified (VS4-1845, Video Scope International) and recorded by a video camera (VarioTrig, PCO computer optics) providing 30 interlaced frames/s. Image sequences were stored on an optical disc recorder (OMDR, Panasonic TQ-3038F).

To assure precise timing of image collection relative to the voltage pulse in some experiments, the "grab out" signal from the free-running video camera was used as a time reference. When the EPC-9 was triggered to start signal acquisition, it waited for the next grab out signal and then, after a fixed but adjustable delay, sent a signal enabling image acquisition by the OMDR. Since the OMDR was time-locked to the grab out signal, its first acquired video frame always followed the signal from the EPC-9 with the same delay. A second EPC-9 signal given 2 ms later triggered the opening of the shutter in the laser light path. Voltage pulses were precisely timed to start 8 ms before the period over which the camera collected light for the 13th half frame of a sequence of images. The timing of the pulse was confirmed in parallel experiments by having it power a light-emitting diode (LED). The camera reported the LED light always in exactly the same two video half frames (13 and 14). Moreover, the step applied to the LED in Figure 4C reproduced the waveform shown there without measurable jitter. Using an LED and a photomultiplier, we measured the lag time of the intensifier phosphor. It was 0.63 ms after the LED turned on and 0.60 ms after the LED turned off.

In most experiments, excitation light was polarized in parallel (p polarized) to the plane of incidence, defined as that plane normal to the coverslip which contains the excitation beam. This generates an evanescent field whose electric field vector has two components, one oscillating perpendicular and the other parallel to the coverslip. In our system, the perpendicular is 1.8 times as large as the parallel component (Hellen et al., 1988; Sund et al., 1999). Since the illumination intensity is proportional to the square of the electric field, there is 3.2 times more illumination perpendicular than parallel. To make excitation s polarized, a quarter-wave plate was sometimes placed in the excitation beam prior to entering the microscope. This generates an evanescent field whose electric vector oscillates exclusively parallel to the coverslip.

Data Analysis

Data from the OMDR were digitized using MetaMorph (Universal Imaging) and analyzed with Metamorph and Matlab (Mathworks Inc.). Generally, video frames were de-interlaced into half frames in order to improve time resolution. Video clips with fusing vesicles were visually selected and square regions approximately centered on the vesicle were excised for analysis using Matlab subroutines.

In many experiments, we analyzed vesicle images by plotting their fluorescence against distance from the vesicle center (radial sweep). First, the center of a vesicle was found with subpixel accuracy by fitting a two-dimensional Gaussian function to its image; the amplitude, width, and coordinates in the image plane were the free parameters. Next, circles were drawn around the center with diameters spaced in increments of 1 pixel unit (87.3 nm). For each, fluorescence at 6333 evenly spaced points around the circle was measured and averaged. Many of these measurements fell into the same pixel, and some pixels contributed more measurements than others. Each circle contributes one measurement in a plot of fluorescence intensity as a function of r, the distance from the center. The value at $r = 0$ was the pixel value of the center. Other forms of analysis are described in the text.

Acknowledgments

We thank Drs. W. Betz, H. von Gersdorff, and our colleagues in the lab for their helpful comments on the manuscript. This work was supported by NIH grant MH60600. D.Z. was supported by an NIH Neuroendocrine Training Grant.

Received: March 14, 2002
Revised: August 6, 2002

References

Albillos, A., Dernick, G., Horstmannn, H., Almers, W., Alvarez de Toledo, G., and Lindau, M. (1997). The exocytic event in chromaffin cells revealed by patch amperometry. Nature *389*, 509–512.

Ales, E., Tabares, L., Poyato, J.M., Valero, V., Lindau, M., and Alvarez de Toledo, G. (1999). High calcium concentrations shift the mode of exocytosis to the kiss-and-run mechanism. Nat. Cell Biol. *1*, 40–44.

Axelrod, D. (2001). Selective imaging of surface fluorescence with very high aperture microscope objectives. J. Biomed. Opt. *6*, 6–13.

Betz, W.J., and Bewick, G.S. (1992). Optical analysis of synaptic vesicle recycling at the frog neuromuscular junction. Science *255*, 200–203.

Betz, W.J., Mao, F., and Smith, C.B. (1996). Imaging exocytosis and endocytosis. Curr. Opin. Neurobiol. *6*, 365–371.

Bloom, J.A., and Webb, W.W. (1983). Lipid diffusibility in the intact erythrocyte membrane. Biophys. J. *42*, 295–305.

Bruns, D., and Jahn, R. (1995). Real-time measurement of transmitter release from single synaptic vesicles. Nature *377*, 62–65.

Chernomordik, L.V., Frolov, V.A., Leikina, E., Bronk, P., and Zimmerberg, J. (1998). The pathway of membrane fusion catalyzed by influenza hemagglutinin: restriction of lipids, hemifusion and lipidic fusion pore formation. J. Cell Biol. *140*, 1369–1382.

Crank, J. (1970). The Mathematics of Diffusion (Oxford University Press).

Fernandez, J.M., Neher, E., and Gomperts, B.D. (1984). Capacitance measurements reveal stepwise fusion events in degranulating mast cells. Nature *312*, 453–455.

Fesce, R., Grohovaz, F., Valtorta, F., and Meldolesi, J. (1994). Neurotransmitter release: fusion or 'kiss and run.' Trends Cell Biol. *4*, 1–3.

Gingell, T., and Todd, I. (1979). Interference reflection microscopy. A quantitative theory for image interpretation and its application to cell-substratum separation measurement. Biophys. J. *26*, 507–527.

Gomis, A., Burrone, J., and Lagnado, L. (1999). Two actions of calcium regulate the supply of releasable vesicles at the ribbon synapse of retinal bipolar cells. J. Neurosci. *19*, 6309–6317.

Heidelberger, R., and Matthews, G. (1992). Calcium influx and calcium current in single synaptic terminals of retinal bipolar neurons. J. Physiol. *207*, 623–633.

Heidelberger, R., Heinemann, C., Neher, E., and Matthews, G. (1994). Calcium dependence of the rate of exocytosis in a synaptic terminal. Nature *371*, 513–515.

Hellen, E.H., Fulbright, R.M., and Axelrod, D. (1988). Total internal reflection fluorescence: theory and applications at biosurfaces. In Spectroscopic Membrane Probes, L. Loew, ed. (Boca Raton, FL: CRC Press), pp. 47–79.

Henkel, A.W., and Almers, W. (1996). Fast steps in exocytosis and endocytosis studied by capacitance measurements in endocrine cells. Curr. Opin. Neurobiol. *6*, 350–357.

Henkel, A.W., and Betz, W.J. (1995). Staurosporine blocks evoked release of FM1–43 but not acetylcholine from frog motor nerve terminals. J. Neurosci. *15*, 8246–8258.

Heuser, J.E., and Reese, T.S. (1973). Evidence for recycling of synaptic vesicle membrane during transmitter release at the frog neuromuscular junction. J. Cell Biol. *57*, 315–344.

Jahn, R., and Südhof, T.C. (1999). Membrane fusion and exocytosis. Annu. Rev. Biochem. *68*, 863–911.

Jacobson, K., Hou, Y., Derzko, Z., Wojcieszyn, J., and Organisciak, D. (1981). Lipid lateral diffusion in the surface membrane of cells and in multibilayers formed from plasma membrane lipids. Biochemistry *20*, 5268–5275.

Kavalali, E.T., Klingauf, J., and Tsien, R.W. (1999). Properties of fast

endocytosis at hippocampal synapses. Philos. Trans. R. Soc. Lond. B Biol. Sci. *354*, 337–346.

Klingauf, J., Kavalali, E.T., and Tsien, R.W. (1998). Kinetics and regulation of fast endocytosis at hippocampal synapses. Nature *394*, 581–585.

Klyachko, V.A., and Jackson, M.B. (2002). Capacitance steps and fusion pores of small and large-dense-core vesicles in nerve terminals. Nature *418*, 89–92.

Meldolesi, J., and Ceccarelli, B. (1981). Exocytosis and membrane recycling. Philos. Trans. R. Soc. Lond. B Biol. Sci. *296*, 55–65.

Mennerick, S., and Matthews, G. (1996). Ultrafast exocytosis elicited by calcium current in synaptic terminals of retinal bipolar neurons. Neuron *17*, 1241–1249.

Mennerick, S., Zenisek, D., and Matthews, G. (1997). Static and dynamic properties of large-terminal bipolar cells from goldfish retina: experimental test of a compartment model. J. Neurophysiol. *78*, 51–62.

Monck, J.R., Alvarez de Toledo, G., and Fernandez, J.M. (1990). Tension in secretory granule extensive membrane transfer through the exocytotic fusion pore. Proc. Natl. Acad. Sci. USA *87*, 7804–7808.

Neves, G., and Lagnado, L. (1999). The kinetics of exocytosis and endocytosis in the synaptic terminal of goldfish retinal bipolar cells. J. Physiol. *515*, 181–202.

Peters, C., Bayer, M.J., Buhler, S., Andersen, J.S., Mann, M., and Mayer, A. (2001). Trans-complex formation by proteolipid channels in the terminal phase of membrane fusion. Nature *409*, 581–588.

Pyle, J.L., Kavalali, E.T., Piedras-Renteria, E.S., and Tsien, R.W. (2000). Rapid reuse of readily releasable pool of vesicles at hippocampal synapses. Neuron *28*, 221–231.

Rouze, N.C., and Schwartz, E.A. (1998). Continuous and transient vesicle cycling at a ribbon synapse. J. Neurosci. *18*, 8614–8624.

Richards, D.A., Guatimosin, C., and Betz, W.J. (2000). Two endocytic recycling routes selectively fill two vesicle pools in frog motor nerve terminals. Neuron *27*, 551–559.

Ryan, T.A. (2001). Presynaptic imaging techniques. Curr. Opin. Neurobiol. *11*, 544–549.

Ryan, T.A., Reuter, H., Wendland, B., Schweitzer, F.E., Tsien, R.W., and Smith, S.J. (1993). The kinetics of synaptic vesicle recycling measured at single presynaptic boutons. Neuron *11*, 713–724.

Ryan, T.A., Smith, S.J., and Reuter, H. (1996). The timing of synaptic vesicle endocytosis. Proc. Natl. Acad. Sci. USA *93*, 5567–5571.

Sankaranarayanan, S., and Ryan, T.A. (2000). Real-time measurements of vesicle-SNARE recycling in synapses of the central nervous system. Nat. Cell Biol. *2*, 197–204.

Schikorski, T., and Stevens, C.F. (2001). Morphological correlates of functionally defined synaptic vesicle populations. Nat. Neurosci. *4*, 391–395.

Schmoranzer, J., Goulian, M., Axelrod, D., and Simon, S.M. (2000). Imaging constitutive exocytosis with total internal reflection fluorescence microscopy. J. Cell Biol. *149*, 23–32.

Slepnev, V.I., and De Camilli, P. (2000). Accessory factors in clathrin-dependent synaptic vesicle endocytosis. Nat. Rev. Neurosci. *1*, 151–172.

Smith, C.B., and Betz, W.J. (1996). Simultaneous independent measurement of endocytosis and exocytosis. Nature *380*, 531–534.

Spruce, A.E., Breckenridge, L.J., Lee, A.K., and Almers, W. (1990). Properties of the fusion pore that forms during exocytosis of a mast cell secretory vesicle. Neuron *4*, 643–654.

Stevens, C.F., and Tsujimoto, T. (1995). Estimates for the pool size of releasable quanta at a single central synapse and for the time required to refill the pool. Proc. Natl. Acad. Sci. USA *92*, 846–849.

Stevens, C.F., and Williams, J.H. (2000). "Kiss and run" exocytosis at hippocampal synapses. Proc. Natl. Acad. Sci. USA *97*, 12828–12833.

Steyer, J.A., Horstmann, H., and Almers, W. (1997). Transport, docking and exocytosis of single secretory granules in live chromaffin cells. Nature *388*, 474–478.

Steyer, J.A., and Almers, W. (2001). A real-time view of life within 100 nm of the plasma membrane. Nat. Rev. Mol. Cell Biol. *2*, 268–275.

Sund, S.E., Swanson, J.A., and Axelrod, D. (1999). Cell membrane orientation visualized by polarized total internal reflection fluorescence. Biophys. J. *77*, 2266–2283.

Thomas, P., Lee, A.K., Wong, J.G., and Almers, W. (1994). A triggered mechanism retrieves membrane in seconds after Ca^{2+}-stimulated exocytosis in single pituitary cells. J. Cell Biol. *124*, 667–675.

Torri-Tarelli, F., Grohovaz, R., Fesce, R., and Ceccarelli, B. (1985). Temporal coincidence between synaptic vesicle fusion and quantal secretion of acetylcholine. J. Cell Biol. *101*, 1386–1399.

Tse, F.W., Iwata, A., and Almers, W. (1993). Membrane flux through the pore formed by a fusogenic viral envelope during cell fusion. J. Cell Biol. *121*, 543–551.

Tsuboi, T., Zhao, C., Terakawa, S., and Rutter, G.A. (2000). Simultaneous evanescent wave imaging of insulin vesicle membrane and cargo during a single exocytic event. Curr. Biol. *10*, 1307–1310.

Valtorta, F., Fesce, R., Grohovaz, F., Haimann, C., Hurlbut, W.P., Iezzi, N., Torri-Tarelli, F., Villa, A., and Ceccarelli, B. (1990). Neurotransmitter release and synaptic veiscle recycling. Neuroscience *35*, 477–489.

Valtorta, F., Meldolesi, J., and Fesce, R. (2001). Synaptic vesicles: is kissing a matter of competence? Trends Cell Biol. *11*, 324–328.

Verstreken, P., Kjaerulff, O., Lloyd, T.E., Atkinson, R., Zhou, Y., Meinertzhagen, I.A., and Bellen, H.J. (2002). Endophilin mutations block clathrin-mediated endocytsois but not neurotransmiter release. Cell *109*, 101–112.

von Gersdorff, H., and Matthews, G. (1994). Dynamics of synaptic vesicle fusion and membrane retrieval in synaptic terminals. Nature *367*, 735–739.

von Gersdorff, H., and Matthews, G. (1997). Depletion and replenishment of vesicle pools at a ribbon-type synaptic terminal. J. Neurosci. *17*, 1919–1927.

von Gersdorff, H., Vardi, E., Matthews, G., and Sterling, P. (1996). Evidence that vesicles on the synaptic ribbon of retinal bipolar neurons can be rapidly released. Neuron *16*, 1221–1227.

von Gersdorff, H., Sakaba, T., Berglund, K., and Tachibana, M. (1998). Submillisecond kinetics of glutamate release from a sensory synapse. Neuron *21*, 1177–1188.

Zenisek, D., Steyer, J.A., and Almers, W. (2000). Transport, capture and exocytosis of single synaptic vesicles at active zones. Nature *406*, 849–854.